JURNAL KIMIA VALENSI
p-ISSN: 2460-6065; e-ISSN: 2548-3013
Journal homepage: https://journal.uinjkt.ac.id/index.php/valensi
Research Article

Preparation and Characterization of Pt/TiO₂ Nanotube Arrays (TNAs) Cathode by Photoreduction Method for Hydrogen Evolution

Sherly Kasuma Warda Ningsih[1,2], Rahmat Wibowo[1], Jarnuzi Gunlazuardi[1]

[1]*Department of Chemistry, Faculty of Mathematics and Natural Sciences, Universitas Indonesia, Depok 16424, Indonesia*
[2]*Department of Chemistry, Faculty of Mathematics and Natural Sciences, Universitas Negeri Padang, Kampus Air Tawar, Padang 25132, Indonesia*

**Email: sherly14@fmipa.unp.ac.id*

Article Info
Received: Sept 13, 2025
Revised: Oct 7, 2025
Accepted: Nov 7, 2025
Online: Nov 30, 2025

Citation:
Ningsih, S. K. W., Wibowo, R., & Gunlazuardi, J. (2025). Preparation and Characterization of Pt/TiO_2 Nanotube Arrays (TNAs) Cathode by Photoreduction Method for Hydrogen Evolution. *Jurnal Kimia Valensi*, 11(2), 179-186.

Doi:
10.15408/jkv.v11i2.46475

Abstract
TiO_2 nanotube arrays were fabricated using a two-step anodization method. TNAs have been modified by the photoreduction technique with Pt as the cathode in the photoelectrocatalytic zone for the reduction reaction of H^+ to produce hydrogen. TNAs with Pt were modified using H_2PtCl_6 as the precursor by immersion of this solution on the TNA substrate. Pt/TNAs were characterized using SEM-EDX, UV-Vis DRS, XRD, Raman Spectroscopy, Photoluminescence (PL), and photoelectrochemical analysis. The results show that the morphology of TNAs in the tube forms 2.1μm in height, and Pt nanoparticles are formed on the mouth wall of the tube with a size of approximately 10nm. EDX analysis shows that the composition of Pt/TNAs is approximately 0.15%, Ti 37.09%, and O 62.76%, indicating that Pt has been decorated on the TNAs photoanode. The band gap of Pt/TNAs was 2.82 eV. The diffractogram shows three groups of diffraction peaks, indicating the presence of anatase TiO_2, Ti as a substrate, and Pt, which has been modified in the TNAs. The Raman peaks of TNAs are confirmed to appear at Raman shifts of 144.75, 196.51, 395.94, 517.14, and 638.85 cm^{-1}. PEC cathodes for hydrogen production using Pt-decorated TNAs have been successfully prepared using photoreduction.

Keywords: Cathode, photoelectrocatalytic, photoreduction, Pt, TNAs

1. INTRODUCTION

Sustainable, carbon-free, and high-efficiency hydrogen production systems at a low cost are urgently needed on an industrial scale. Solar energy for hydrogen production from water sources can overcome the problems of clean energy supply and sustainability of fuel sources, as well as reduce environmental pollution[1,2]. Hydrogen can also be produced through water electrolysis, where hydrogen is produced simultaneously at the cathode and oxygen at the anode. However, water electrolysis [3,4] the process for hydrogen production has the disadvantage of requiring large amounts of electrical energy from non-renewable sources [5,6].

Hydrogen production from water (water splitting) through photoelectrochemistry (PEC) is promising because it is environmentally friendly. Hydrogen production using the PEC technique was first carried out by Fujishima and Honda [7] in 1972, using a TiO_2 semiconductor photoanode and a platinum cathode. This PEC method is a promising pathway for converting solar energy into hydrogen fuel (solar hydrogen) [8,9].

TiO_2 has various morphologies, such as nanorods, films, nanoparticles, and nanotubes [10]. TNAs are one-dimensional (1D) semiconductor materials [11] that exhibit excellent photocatalytic properties as photoelectrodes and good physicochemical stability [12,13,14]. This is because the TNAs material has a large specific surface area [15,10], and an open 1D channel for charge transport, so that it will reduce the occurrence of recombination between electrons (e) and holes (h^+). The photocatalytic performance of this 1D material is better because there is an increase in quantum charge caused by an almost linear transmission path for electrons, so it can shorten the electron transport distance and reduce charge recombination [16].

TNAs can be prepared using various methods, such as hydrothermal, template, and anodization techniques [15,17,18,19]. The anodization method has the advantages of being simple, low-cost, and easy to control the reaction rate in forming tubes with a highly ordered arrangement. The one-step anodization method has the disadvantage that the surface of the resulting nanotubes is less smooth and less highly ordered [20,21]. TNAs were first prepared using a two-step anodization method by Wang in 2009 [22]. The resulting TNAs are smoother and more highly ordered [23] to overcome the problem of rough TNAs tube surfaces that are easily removed from the titanium matrix using the one-step anodization method [21].

TNAs have a larger band gap (3.2 eV) and only respond to UV light. Much research is being done on modifying TNAs for responsivity to visible light through metal doping, such as Ag [24], Ag and Au codoped [25], Fe [26], and Pt [27]. TNAs can also be modified with nonmetals [28,28,29], and heterojunction modification [30,31,32]. In this study, we synthesized Pt-decorated TNAs using the photoreduction method. TNAs as a substrate was synthesized by two-step anodization with an increased second voltage. Pt/TNAs were used as cathodes for hydrogen evolution.

2. RESEARCH METHODS

Materials and Instrumentations

The materials used were Ti foil, NH_4F, ethylene glycol, deionized water, H_2PtCl_6, methanol, ethanol, acetone, KOH, and sandpaper. The instrumentations used were Scanning Electron Microscopy- Energy Dispersive X-ray (SEM-EDX), Ultraviolet Visible Spectroscopy, X-ray Diffraction, Raman Spectroscopy, Photoluminescence, Linear Sweep Voltammetry (LSV), and Multi-Pulsed Amperometry (MPA).

Fabrication of TNAs by Two-Step Anodization Method [33,34].

Titanium (Ti) foil was first cleaned with sandpaper in sizes 1000 and 1500 cc. The Ti foil was then cleaned using a soap solution to remove impurities. Subsequently, it was sonicated in acetone (technical grade), ethanol (technical grade), and distilled water for 16 minutes each, and then the foil was dried in an open place. All anodization processes were carried out in an electrochemical cell with two electrodes. The Ti foil was used as the working electrode and the stainless-steel plate as the counter electrode. The electrolyte was an ethylene glycol solution containing 0.3% NH_4F and 2% H_2O. The distance between the two electrodes was set at 1.5 cm. The Ti foil was anodized using the two-step anodization method. In the first stage, anodization was carried out at potential variations of 40 V for 60 min. The results of anodization in the first stage were removed by sonication in distilled water for 20 minutes and dried in an open place to obtain a template for the second stage anodization. The second stage anodization was carried out by increasing the anodization potential to 50 V for 15, 30, and 60 minutes. The anodized Ti foil was rinsed with distilled water and dried in an open place. Furthermore, it was calcined at 450 °C for 2 h in an air (a heating rate of 5 °C/min).

Preparation of Pt/TNAs Cathode with Modification by Photoreduction Method [35]

Pt-decorated TNAs samples were prepared using a photoreduction method on TNAs foil. The TNAs film was immersed in H_2PtCl_6 solution (2 g/L) for 20 min, then rinsed with distilled water and dried in air. The TNAs film was then immersed in a 20% methanol solution and irradiated with a UV lamp with a 2 × 15 W power for 30 min to reduce Pt^{2+} to Pt^0. The samples were characterized using Scanning Electron Microscopy-Energy Dispersive X-ray (SEM-EDX), Ultraviolet-Visible Spectroscopy, X-ray Diffraction, Raman Spectroscopy, Photoluminescence, Linear Sweep Voltammetry (LSV), and Multi-Pulsed Amperometry (MPA).

3. RESULTS AND DISCUSSION

Electron transfer from the conduction band (CB) can produce hydrogen, and hole transfer from the valence band (VB) can oxidize water. Hydrogen production using unmodified TiO_2 produces very little hydrogen [36]. Therefore, TNAs modification was carried out using Pt metal with a photoreduction method functioning as a PEC cathode that serves as a catalysis zone where the reduction reaction of H^+ to hydrogen occurs. Pt modification on TNAs was carried out using a hexachloroplatinum precursor solution (H_2PtCl_6). The TNAs photoanode was dipped with H_2PtCl_6 solution until evenly distributed. This TNAs photoanode was then dried, rinsed with distilled water, and inserted into a 20% methanol solution while irradiating with UV light (black light) with a power of 2×15 W for 30 minutes. Electrons from TiO_2 photoexcitation were used to reduce Pt^{4+} ions to platinum (Pt^0).

The surface morphology and cross-sectional image of Pt/TNAs are shown in **Figure 1**. The image shows that Pt nanoparticles are present on the wall of the TNAs surface tube (**Figure 1a**). The diameter of the TNAs tube is approximately 50.15 nm, and the length of the tube is approximately 2.1 µm (**Figure 1b**). In this SEM image, it can be seen that Pt nanoparticles are formed on the mouth wall of the tube, which is a very small size of approximately 10 nm. From the results of this cross-section test, it can be seen that the TNAs tube is more highly ordered. EDX analysis was carried out to determine the composition of Pt/TNAs. **Figure 1c** shows that the percentage of Pt atoms is approximately 0.15%, Ti 37.09%, and O 62.76%. This indicates that Pt has been decorated on the TNAs photoanode.

The UV-Vis DRS spectra of Pt samples decorated on TNAs with variations in the second-stage anodization time of 15 minutes, 30 minutes, and 60 minutes are shown in **Figure 2**. The spectra show a redshift in absorption at a wavelength of approximately 390 nm. The band gap value of Pt/TNAs was calculated using the Kubelka-Munk equation, and the Tauc plot gives a band gap value of approximately 2.82 eV. The band gap value of TiO_2 decreases with the presence of Pt, indicating the Pt/TNAs material responds to visible light (redshift). The presence of Pt also facilitates electron transfer from TiO_2 to the metal. The band gap obtained for Pt/TiO_2 also follows the literature [37].

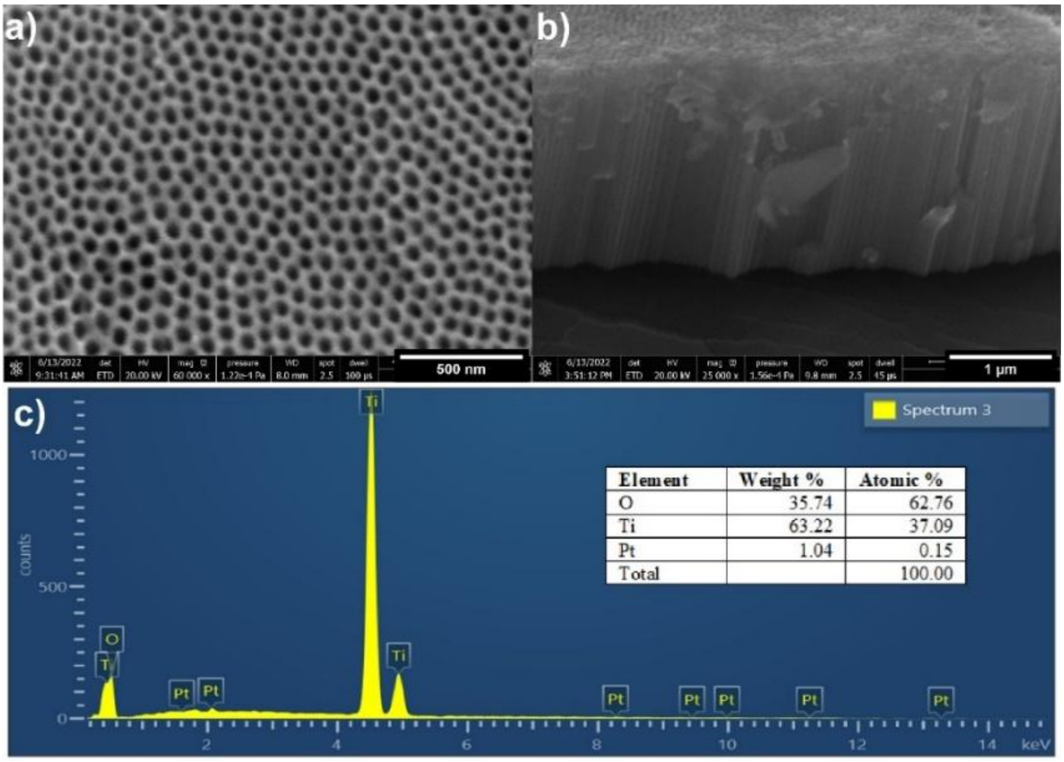

Element	Weight %	Atomic %
O	35.74	62.76
Ti	63.22	37.09
Pt	1.04	0.15
Total		100.00

Figure 1. SEM Photos of a) Surface of Pt/TNAs, b) Cross Section of Pt/TNAs, and c) EDX of Pt/TNAs

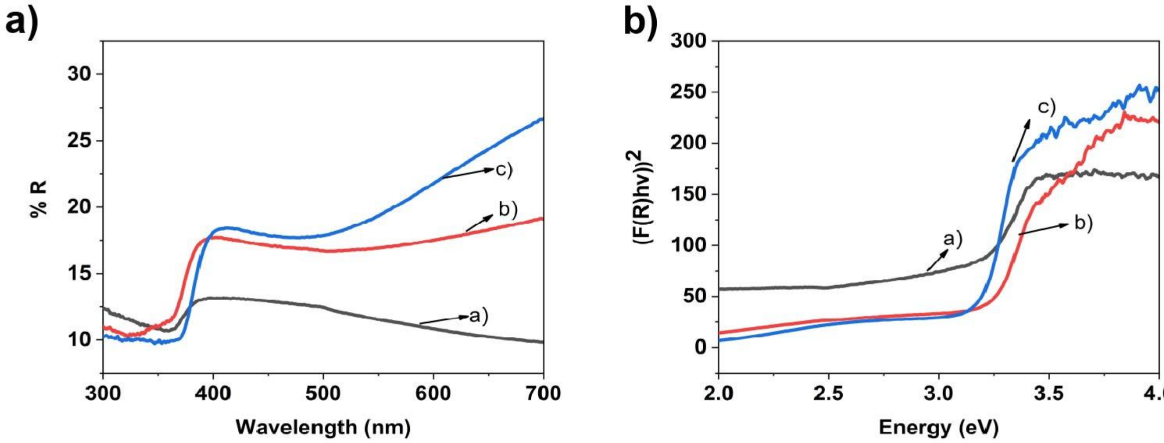

Figure 2. A Spectra of UV-Vis DRS and B Tauc Plot of Pt decorated on a) TNAs 40 V for 60 min at one step and 50 V for 15 min at the second step, b) 40 V for 60 min, 50 V for 30 min, c) 40 V for 60 min, 50 V for 60 min

The diffractograms of the synthesized TNAs and Pt/TNAs are shown in **Figure 3**. The diffractogram shows three groups of diffraction peaks indicating the presence of anatase TiO_2, Ti as a substrate, and Pt modified on the TNAs. The diffraction peaks of anatase TiO_2 can be observed at 2θ: 25.33°; 38.44°; 48.18°; 54.02°; 55.12°; 70.71° and 76.28°, respectively, with Miller indices (101), (004), (200), (105), (211), (220) and (301). These seven diffraction peaks follow the JCPDS standard No. 00-021-1272 with the anatase phase [38]. In addition to this anatase peak, Ti metal peak is also observed, consistent with the JCPDS standard No. 21-1294, at 2θ: 35.11° and 40.20°, corresponding to the Miller indices (100) and (101). TiO_2 nanotubes are typically synthesized by anodizing Ti metal (foil or thin film). The resulting TiO_2 layer does not cover the entire substrate volume; it is typically only a few micrometers thick. The diffractogram shows Pt peaks at 2θ: 38.44°, 68.77°, and 82.35°, corresponding to the Miller indices (111), (220), and (222), respectively. This follows the ICSD standard No. 01-087-0647 with a cubic crystal phase. The appearance of these peaks confirms that Pt has been deposited in crystalline metallic form on the TiO_2 surface. The relatively low intensity and broadening of the peaks indicate that the Pt particle size is very small (in the nanometer scale). This cubic structure of Pt plays an important role in facilitating electron transfer from TiO_2 to Pt, forming a Schottky barrier that enhances the efficiency of photocatalytic charge separation.

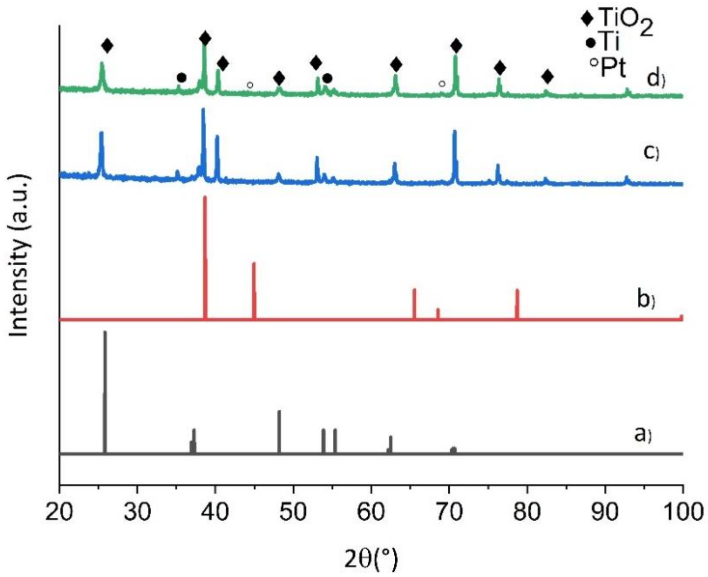

Figure 3. Diffractograms of a) TiO_2 Standard, b) Pt Standard, c) TNAs, and d) Pt decorated on TNAs

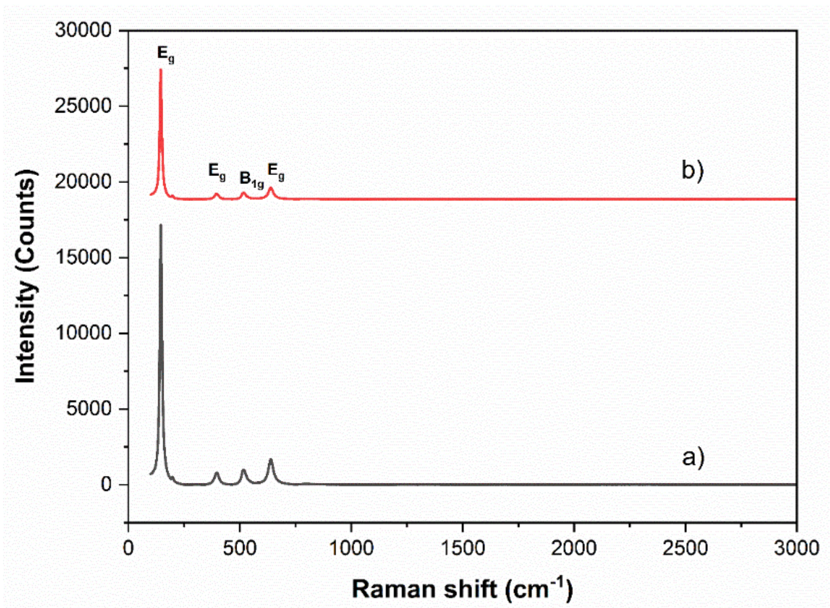

Figure 4. Raman Spectra of a) TNAs and b) Pt/TNAs

Figure 4 shows the Raman spectra of bare TNAs and TNAs decorated with Pt. This Raman analysis was performed using a laser beam with a wavelength of 525 nm. The Raman peaks of TNAs are confirmed to appear at Raman shifts of 144.75, 196.51, 395.94, 517.14, and 638.85 cm^{-1}, indicating the active Raman phonon modes $E_{g(1)}$, $E_{g(2)}$, $B_{1g(1)}$, $A_{1g(1)}$+ $B_{1g(2)}$, and $E_{g(3)}$, respectively (**Figure 3a**). The Raman peak with the highest intensity at 144.75 cm^{-1} confirms the single crystal of anatase TiO_2 [39]. The Raman peak of Pt/TNAs is similar to that of bare TNAs. However, the typical Raman peak at 145 cm^{-1} has decreased in intensity, indicating that defects occur on the TiO_2 surface with the formation of Schottky barriers. Pt in TNAs does not show other phonon modes, confirming that the addition of Pt to TNAs does not change the phase of TNAs, these results are consistent with the previous report [39].

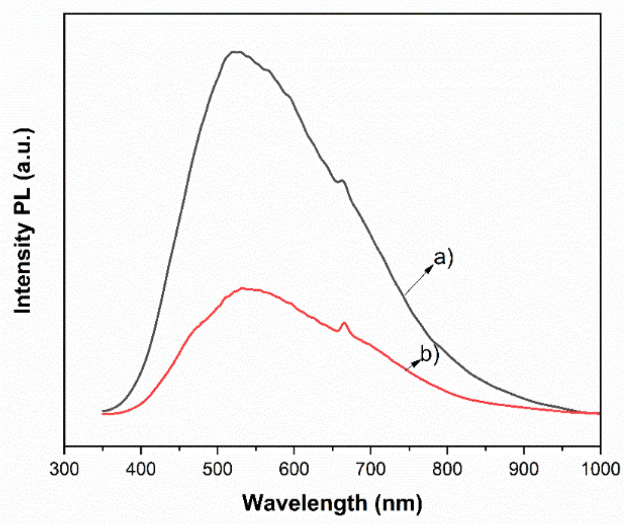

Figure 5. PL Spectra of a) TNAs and b) Pt/TNAs

The PL spectra of TNAs and Pt/TNAs samples are shown in **Figure 5**. The high PL intensity peak indicates that the separation efficiency of photogenerated electron-hole pairs is weaker, and electrons have more difficulty transferring from the conduction to the valence band [40]. The spectra show that the PL intensity of Pt/TNAs prepared on TNAs is lower than that of bare TNAs. This confirms that the higher charge separation efficiency is due to the electric field generated at the Pt/TNAs interface, which is consistent with the previous report [41]. Lower PL intensity upon Pt loading indicates reduced electron-hole recombination (Pt acts as an electron sink/Schottky junction). The PL spectra show that the sharpness of the peak of TNAs modified with Pt becomes broader with a lower PL intensity. Therefore, modifying Pt on TNAs can minimize the recombination rate of TNAs.

Photoelectrochemical Activity Testing of Pt/TNAs Cathode

Platinum (Pt) is a material that has high stability and good catalytic activity in reducing H^+ to hydrogen (H_2). When Pt/TNAs are used as cathodes for hydrogen production, H^+ ions in contact with the Pt surface and those adsorbed on the Pt/TNAs interface are reduced to H_2. The photoelectrochemical activity of Pt/TNAs was tested using the LSV method. The measurements were carried out using a single-compartment photoelectrochemical cell consisting of a three-electrode system: a working electrode in the form of synthetic Pt/TNAs, a reference electrode Ag/AgCl, and a Pt electrode as a counter electrode, all immersed in a 1 M KOH electrolyte solution. The light source used was a 19 W visible LED lamp. The photoelectrochemical performance of Pt/TNAs with variations of the second-stage anodization time was carried out by irradiation with visible light and UV light in a 1 M KOH electrolyte solution. The I-V curve of the synthesized Pt/TNAs electrode is shown in **Figure 6**.

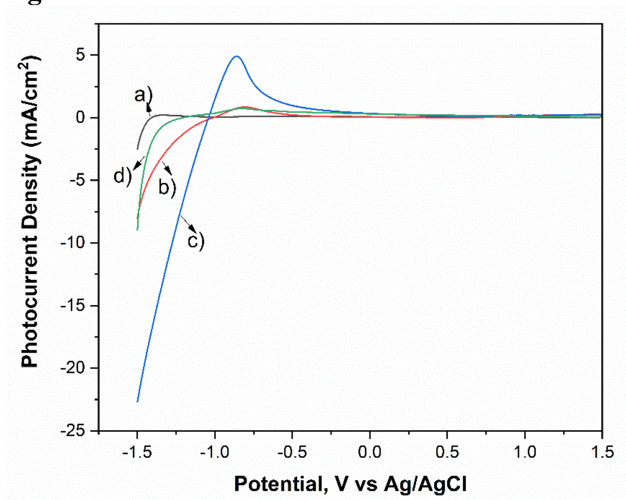

Figure 6. I-V Curve of a) TNAs and b) Pt decorated on TNAs 40 V for 60 min at one step and 50 V for 15 min at the second step, c) Pt decorated on TNAs 40 V for 60 min, 50 V for 30 min, and d) Pt decorated on TNAs 40 V for 60 min, 50 V for 60 min

The curve shows a cathodic current at a potential below -1 V. This cathodic current indicates water reduction on the surface of the Pt/TNAs electrode [35]. The anodic current was observed at a potential above -1 V for this electrode variation. The anodic current value of Pt/TNAs is greater than that of TNAs, which indicates that the presence of Pt metal in TNAs can increase charge separation and reduce electron recombination because electrons migrate to the Pt metal. This is because the Fermi level position of the metal is higher than the Fermi level of the semiconductor. The electrons will flow from the semiconductor to the metal until the Fermi level is at the same level. This Fermi level equalization process will form a boundary layer, because the metal has an excess negative charge, and the semiconductor forms an excess positive charge [42,43].

4. CONCLUSIONS

The characterization of Pt/TNAs showed that Pt has been successfully decorated on TNAs using the photoreduction method. The optimum Pt/TNAs were obtained using TNAs anodized at 40 V for 60 minutes and 50 V for 30 minutes, showing a higher cathodic current response. This optimum Pt/TNAs will be used as a cathode in the PEC section for hydrogen production. Pt is a material that has high stability and good catalytic activity in reducing H^+ to hydrogen (H_2). When Pt/TNAs are used as cathodes for hydrogen production, the H^+ ions in contact with the Pt surface and those adsorbed on the Pt/TNAs interface are reduced to H_2.

REFERENCES

1. Li P, Yan R, Zhang J, Wu M, He Y, Liu T, Wang J. Hybrid hydrogen production system utilizing photovoltaics, photocatalysis, and thermochemistry for effective full-spectrum solar energy harvesting. *Energy Convers Manag*. 2025;336. doi:https://doi.org/10.1016/j.enconman.2025.119884
2. Ahmed M, Dincer I. A review on photoelectrochemical hydrogen production systems: Challenges and future directions. *Int J Hydrogen Energy*. 2019;44(5):2474-2507. doi:10.1016/j.ijhydene.2018.12.037
3. Breuning L, Nigbur F, Wienert P, Khatiwada D. Energy Application of an electrolysis system model for techno-economic optimization of hydrogen production in industry-based case studies. *Int J Hydrogen Energy*. 2025. doi:10.1016/j.ijhydene.2025.03.291
4. Wang X, Wang X, Song Z, Wang Y, Hu J, Zhou L, Zhang L. Ultrasonic assisted electrolysis enables massive production of hydrogen bulk nanobubbles. *J Colloid Interface Sci*. 2025;695(April):137748. doi:10.1016/j.jcis.2025.137748
5. Dou B, Zhang H, Song Y, Zhao L, Jiang B, He M, Ruan C, Chen H, Xu Y. Hydrogen production from the thermochemical conversion of biomass: Issues and challenges. *Sustain Energy Fuels*. 2019;3(2):314-342. doi:10.1039/c8se00535d
6. Gao X, Li C, Lv T, Jiao F, Chen F. Electrolytic hydrogen production and energy conversion performance based on non-imaging solar system constructed with congruent concentrating surface. *Renew Energy*. 2025;248(October 2024):123136. doi:10.1016/j.renene.2025.123136
7. Fujishima A, Honda K. Electrochemical photolysis of water at a semiconductor electrode. *Nature*. Published online 1972. doi:10.1038/238037a0
8. Srimurugan V, Suryakumar C, Jha S, Raj CC, Prasanth R. Synergistic effects of MoS_2/TiO_2 nanotubes p-n heterojunction photoelectrode for hydrogen evolution. *Int J Hydrogen Energy*. 2025;103(January):609-623. doi:10.1016/j.ijhydene.2025.01.230
9. Kong D, Qi J, Liu D, Zhang X, Pan L, Zou J. Ni-Doped - $BiVO_4$ with - V4+ Species and Oxygen Vacancies for Efficient Photoelectrochemical Water Splitting. *Trans Tianjin Univ*. 2019;25(4):340-347. doi:10.1007/s12209-019-00202-1
10. Min SK, Cho K, Yoon J, Choi W. Photoelectrochemical Degradation of Organic Compounds Coupled with Molecular Hydrogen Generation Using Electrochromic TiO_2 Nanotube Arrays. *Environ Sci Technol*. 2017;51(11):6590-6598. doi:10.1021/acs.est.7b00774
11. Huo K, Gao B, Fu J, Chu PK. Fabrication, modification, and biomedical applications of anodized TiO_2 nanotube arrays. *RSC Adv*. 2014;4:17300-17324. doi:10.1039/c4ra01458h
12. Yu R, Liu Z, Pourpoint F, Armstrong AR, Grey CP, Bruce PG. Nanoparticulate TiO_2 (B): An Anode for Lithium-Ion Batteries. *Angewandte*. 2012;51:2164-2167. doi:10.1002/anie.201108300
13. Deng Y, Zhanfong M, Fengzhang R, Guangxin W. Enhanced photoelectrochemical performance of TiO_2 nanorod array films based on TiO2 compact layers synthesized by a two-step method. *RSC Adv*. 2019;9:21777-21785. doi:10.1039/c9ra03755a
14. Shaodong S, Song P, Cui J, Liang S. Amorphous TiO_2 nanostructures: synthesis, fundamental properties and photocatalytic applications. *Catal Sci Technol*. Published online 2019. doi:10.1039/C9CY01020C
15. Hailiang L, Wang G, Niu J, Wang E, Niu G, Xie C. Preparation of TiO_2 nanotube arrays with efficient photocatalytic performance and super-hydrophilic properties utilizing anodized voltage method. *Results Phys*. 2019;14(July):102499. doi:10.1016/j.rinp.2019.102499
16. Liu J, Yao M, Shen L. The Third Generation Photovoltaic Cells Based on Photonic Crystals. *Mater Chem C*. Published online 2019. doi:10.1039/C8TC05461D
17. Wu L, Li C, Song Y, Zhang K, Zhang J, Li P,

Zhu X. What happens if anodic TiO_2 nanotubes are soaked in H_3PO_4 at room temperature for a long time? *Electrochem commun*. 2019;105(July):106501. doi:10.1016/j.elecom.2019.106501
18. Yi Z, Zeng Y, Wu H, Chen X, Fan Y, Yang H, Tang Y, Yi Y, Wang J, Wu P. Synthesis, surface properties, crystal structure and dye-sensitized solar cell performance of TiO_2 nanotube arrays anodized under different parameters. *Results Phys*. 2019;15(August):102609. doi:10.1016/j.rinp.2019.102609
19. Niu D, Han A, Cheng H, Ma S, Tian M, Liu L. Effects of organic solvents in anodization electrolytes on the morphology and tube-to-tube spacing of TiO_2 nanotubes. *Chem Phys Lett*. 2019;735(August):136776. doi:10.1016/j.cplett.2019.136776
20. Zang Z, Wang P. Optimization of photoelectrochemical water splitting performance on hierarchical TiO2 nanotube arrays. *Energy Environ Sci*. 2012;5(4):6506-6512. doi:10.1039/c2ee03461a
21. Siyu C, Zhang S, Tan Z, Zhang S. *Effect of Two-Step Anodization on Structure of TiO_2 Nanotube Arrays*. Springer Singapore; 2018. doi:10.1007/978-981-13-0110-0
22. Daoai W, Yu B, Wang C, Zhou F, Liu W. A novel protocol toward perfect alignment of anodized TiO_2 nanotubes. *Adv Mater*. 2009;21(19):1964-1967. doi:10.1002/adma.200801996
23. Hongjun W, Zhang Z. Photoelectrochemical water splitting and simultaneous photoelectrocatalytic degradation of organic pollutant on highly smooth and ordered TiO_2 nanotube arrays. *J Solid State Chem*. 2011;184(12):3202-3207. doi:10.1016/j.jssc.2011.10.012
24. Garnica-Romo MG, Mora-Mora Z, Alvarado-Gil JJ, Martínez-Flores HE. Electrochemical nanosensor based on Ag-doped TiO_2 nanotubes for detecting ascorbic acid. *Int J Electrochem Sci*. 2024;19(2):2-11. doi:10.1016/j.ijoes.2024.100481
25. Khairy M, Kamar EM, Mousa MA. Photocatalytic activity of nano-sized Ag and Au metal-doped TiO_2 embedded in rGO under visible light irradiation. *Mater Sci Eng B*. 2022;286(September):116023. doi:10.1016/j.mseb.2022.116023
26. Mir A, Iqbal K, Rubab S, Shah MA. Effect of concentration of Fe-dopant on the photoelectrochemical properties of Titania nanotube arrays. *Ceram Int*. 2022;49(1):677-682. doi:10.1016/j.ceramint.2022.09.037
27. Soundarya TL, Harini R, Manjunath K, Udayabhanu, Nirmala B, Nagaraju G. Pt-doped TiO_2 nanotubes as photocatalysts and electrocatalysts for enhanced photocatalytic H_2 generation, electrochemical sensing, and supercapacitor applications. *Int J Hydrogen Energy*. 2023;48(82):31855-31874. doi:10.1016/j.ijhydene.2023.04.289
28. Szkoda M, Siuzdak K, Lisowska-Oleksiak A. Non-metal doped TiO_2 nanotube arrays for high efficiency photocatalytic decomposition of organic species in water. *Phys E Low-Dimensional Syst Nanostructures*. 2016;84:141-145. doi:10.1016/j.physe.2016.06.004
29. Zhang T, Ni A, Xu Y, Fu D, Lin P. N-doped TiO_2 nanotube arrays with mixed phase for enhanced photocathodic protection of 304 stainless steel under visible light. *J Phys Chem Solids*. 2022;170(July):110923. doi:10.1016/j.jpcs.2022.110923
30. Li Z, Zhang Z, Dong Z, Wu Y, Zhu X, Cheng Z, Liu Y, Wang Y, Zheng Z, Cao X, Wang Y, Liu Y. CuS/TiO_2 nanotube arrays heterojunction for the photoreduction of uranium (VI). *J Solid State Chem*. 2021;303(July):122499. doi:10.1016/j.jssc.2021.122499
31. Jiaqin L, Ruan L, Adeloju SB, Wu Y. BiOI/TiO_2 nanotube arrays, a unique flake-tube structured p–n junction with remarkable visible-light photoelectrocatalytic performance and stability. *J Chem Soc Dalt Trans*. 2014;43(4):1706-1715. doi:10.1039/c3dt52394b
32. Kasuma Warda Ningsih S, Wibowo R, Gunlazuardi J. Photoelectrochemical performance of BiOI/TiO $_2$ nanotube arrays (TNAs) p-n heterojunction synthesized by SILAR-ultrasonication-assisted methods. *R Soc Open Sci*. 2023;10(6). doi:10.1098/rsos.221563
33. Ningsih, S.K.W, Wibowo, Rahmat, Gunlazuardi J. Photoelectrochemical performance of BiOI/TiO_2 nanotube arrays (TNAs) p-n heterojunction synthesized by SILAR-ultrasonication-assisted methods. *R Soc Open Sci*. 2023;10(6). doi:10.1098/rsos.221563
34. Ningsih SKW, Syauqi MI, Wibowo R, Gunlazuardi J. Effect of potential variation on morphology and photoelectrochemical properties of TiO2 nanotube arrays (TNAs) by two-step anodization method. *J Appl Electrochem*. 2024;54(4):739-756. doi:10.1007/s10800-023-01999-5
35. Surahman H. Pengembangan Sel Fotoelektrokimia Menggunakan Elektroda TiO_2 Nanotube Arrays Tersensitasi CdS Nanopartikel Untuk Produksi Hidrogen. In:

Disertasi. ; 2017.
36. Chen X, Qin S, Denisov N, Kure-Chu SZ, Schmuki P. Pt-single atom decorated TiO_2: Tuning anodic TiO_2 nanotube structure and geometry toward a high-performance photocatalytic H_2 production. *Electrochim Acta*. 2023;446(January):142081. doi:10.1016/j.electacta.2023.142081
37. Esrafili A, Salimi M, jonidi jafari A, Reza Sobhi H, Gholami M, Rezaei Kalantary R. Pt-based TiO_2 photocatalytic systems: A systematic review. *J Mol Liq*. 2022;352:118685. doi:10.1016/j.molliq.2022.118685
38. Denisov N, Yoo JE, Schmuki P. Effect of different hole scavengers on the photoelectrochemical properties and photocatalytic hydrogen evolution performance of pristine and Pt-decorated TiO_2 nanotubes. *Electrochim Acta*. 2019;319:61-71. doi:10.1016/j.electacta.2019.06.173
39. Kaur N, Mahajan A, Bhullar V, Singh DP, Saxena V, Debnath AK, Aswal DK, Devi D, Singh F, Chopra S. Fabrication of plasmonic dye-sensitized solar cells using ion-implanted photoanodes. *RSC Adv*. 2019;(9):20375-20384. doi:10.1039/c9ra02657f
40. Ge MZ, Li SH, Huang JY, Zhang KQ, Al-Deyab SS, Lai YK. TiO_2 nanotube arrays loaded with reduced graphene oxide films: Facile hybridization and promising photocatalytic application. *J Mater Chem A*. 2015;3(7):3491-3499. doi:10.1039/c4ta06354f
41. Yang Z, Xu W, Yan B, et al. Gold and Platinum Nanoparticle-Functionalized TiO_2 Nanotubes for Photoelectrochemical Glucose Sensing. *ACS Omega*. 2022;7(2):2474-2483. doi:10.1021/acsomega.1c06787
42. Manuel AP, Shankar K. Hot electrons in TiO_2–noble metal nano-heterojunctions: Fundamental science and applications in photocatalysis. *Nanomaterials*. 2021;11(5). doi:10.3390/nano11051249
43. Kumar A, Choudhary P, Kumar A, Camargo PHC, Krishnan V. Recent Advances in Plasmonic Photocatalysis Based on TiO2 and Noble Metal Nanoparticles for Energy Conversion, Environmental Remediation, and Organic Synthesis. *Nano Micro Small*. 2022;18(1). doi:10.1002/smll.202101638